ORIGINAL PAPER

Rainfall and sea-level variability in the face of changing El Niño: evidence from the U.S.-affiliated Pacific islands

Md. Rashed Chowdhury[1,5] · Pao-Shin Chu[2] · Ousmane Ndiaye[3] · James T. Potemra[4]

Abstract

The prime concerns for future disruptions in the El Niño-Southern oscillation (ENSO)-sensitive U.S.-affiliated Pacific islands (USAPIs) are centered on the consequences of increasing frequency of ENSO and related drought and flooding activities. Recent observations also revealed that island-specific rainfall and sea-level patterns appear to be different during the three types of El Niño events (eastern, mixed, and central Pacific). The primary motivation of the study is to identify the impacts of three different types of El Niño on rainfall and sea-level variability in USAPIs. Results reveal that different types of El Niño can lead to different variations in rainfall and sea level in the USAPIs. While the eastern Pacific and mixed El Niño events are associated with lower than normal rainfall in all USAPIs, the central Pacific El Niño events are found to be associated with enhanced rainfall in many USAPIs. Similarly, while all the USAPIs displayed lower than normal sea level during eastern Pacific and mixed El Niño events, some of the USAPIs displayed higher than normal sea level during central Pacific events. Information related to island-specific rainfall and sea-level response to different El Niño events is critical to support the short-to-mid-term planning and management in climate-sensitive sectors in the USAPIs.

1 Introduction

While long-term decadal variations in climate are increasingly understood to exist (see Irving et al. 2011), our ability to predict such changes in an operational context

✉ Md. Rashed Chowdhury
  rashed@hawaii.edu; rashed.chowdhury@asu.edu

  Ousmane Ndiaye
  http://www.anacim.sn

[1] Pacific ENSO Applications Climate Center (PEAC), Joint Institute for Marine and Atmospheric Research, University of Hawaii at Manoa, Honolulu, HI 96822, USA

[2] Department of Atmospheric Sciences, School of Ocean and Earth Science and Technology (SOEST), University of Hawaii at Manoa, Honolulu, HI 96822, USA

[3] National Civil Aviation and Meteorology Agency, Aéroport Léopold Sédar Senghor, BP: 8184, Dakar, Senegal

[4] International Pacific Research Center, School of Ocean and Earth Science and Technology, University of Hawaii, Honolulu, HI 96822, USA

[5] Present Address: School of Sustainable Engineering and the Built Environment, Arizona State University, Tempe, AZ, USA

(short-to-medium term) is somewhat difficult, particularly for the small islands in the U.S.-affiliated Pacific islands (USAPIs) (see Chowdhury and Chu (2019) for a synthesis of long-term climate change impacts on USAPIs). In contrast, the El Niño-Southern Oscillation's (ENSO) inter-annual time-scale variability and impacts, which are projected to intensify in future, are found to be more effective for developing an immediate response plan for adaptations. Despite the long-term warming signal, the primary concerns for future disruptions in the USAPIs (Fig. 1) are centered on the consequences of the increasing frequency of ENSO and related rainfall, sea level, and other climate variability (Power et al. 2017). The USAPI region is located near the center of activity of the major variations in atmospheric and oceanic circulation associated with ENSO. The impact of ENSO on tropical cyclones (TCs) is also important; however, it is not within the scope of this study (see Lander 1994; Chu 2004; Marler 2014).

The main objective of this study is to synthesize the physical and social impacts of three different types of El Niño: Eastern Pacific El Niño (EPE) or cold tongue El Niño; mixed El Niño (ME); and Central Pacific El Niño (CPE), also warm pool El Niño or El Niño Modoki (Kug et al. 2009; Murphy et al. 2014). The CPE events are becoming more common, a trend that is projected to continue with ongoing
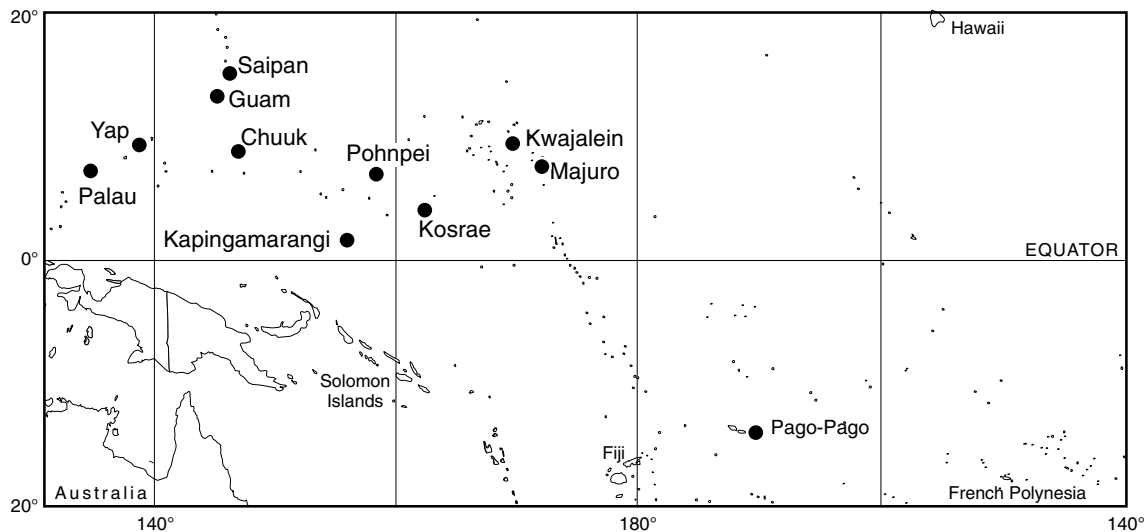
Fig. 1 Locations of U.S.-affiliated Pacific islands (USAPIs); those discussed here are labeled with black dots. The USAPIs are composed of Guam, Commonwealth of the Northern Mariana Islands (CNMI) (Saipan), the Republic of the Marshall Islands (RMI) (Majuro and Kwajalein), and the Federated States of Micronesia (FSM) (Chuuk, Kosrae, Pohnpei, which includes the island of Kapingamarangi, and Yap)

climate change (Freund et al. 2019). Looking at the past four centuries, the most recent 30-year period includes fewer, but more intense, EPE events (Lee and McPhaden 2010; Freund et al. 2019). Wang et al. (2019) showed that since the 1970s El Niño changed its origination from the eastern Pacific to the western Pacific, along with increased strong El Niño events due to a background warming in the western Pacific warm pool. Changes in El Niño's location and intensity under anthropogenic warming are of great importance to society; however, current climate models' projections remain uncertain.

The motivation for this study emerged as recent evidence showed that the island-specific rainfall and sea-level pattern (https://www.weather.gov/peac/update; accessed on May 2019) appear to vary between the three different types of El Niño events (see Ludert et al. 2018). This was unexpected as the apparent rainfall pattern looks only slightly different from previous study by Murphy et al. (2014) where the ME and CPE events are associated with significantly wetter than normal conditions in the same western Pacific islands. However, in contrast to Murphy et al. (2014), some of the USAPIs display significantly lower than normal rainfall during ME and CPE events. Similarly, while lower than normal sea level is clearly visible across the USAPIs during an EPE event, some of the islands experienced elevated sea levels during ME events. These findings are somewhat new and very critical to support the short-to-midterm planning and management in ENSO-sensitive sectors for the USAPI region. It is necessary to expand our understanding on the trend of changing El Niño to understand the relationship between different types of El Niño and island-wide rainfall

and sea-level variations, because this information is essential for hazard management in the USAPIs.

Three El Niño events are classified on the basis of spatial patterns of the sea surface temperature (SST) anomaly during 1970–2019. The anomalies are averaged from September to the following February and discussed further in Sect. 4 (see Kug et al. 2009). The EPE event is characterized by relatively large SST anomalies in the Niño-3 region (5° S–5° N, 90–150° W). The ME is linked to SST anomalies bounded by Niño-3.4 region (5° S–5° N, 170°–120° W), and the CPE event is connected to SST anomalies in the Niño-4 region (5° S–5° N, 160° E–150° W). The SST pattern of the EPE event is quite similar to that of the conventional El Niño (Rasmusson and Carpenter 1982) and the SST pattern in the CPE is similar to Fang and Mu (2018) (also see Freund et al. 2019; Lu et al. 2020). The main focus of this work is centered on El Niño-impacts as the frequency of extreme El Niño events doubles under the 1.5 °C Paris target, while extreme La Niña events see little change at either 1.5° or 2 °C warming (Guojian et al. 2017). Therefore, from a disaster risk reduction perspective, the El Niño-induced hazards need immediate attention in the USAPIs (also see Kelman 2019).

2 Data, basic indices, and methods

SST and wind indices for different (EP, ME, CP) El Niño years: The Extended Reconstructed SST (ERSST: version 4) (Comprehensive Ocean–Atmosphere Data) data from the National Oceanic and Atmospheric Administration

(NOAA)-National Center for Environmental Information (NCEI) is used. The SST data for the tropical region extend from 35° S to 35° N and 100° E to 60° W. The research and development application tool of the 'Physical Sciences Laboratory' of NOAA (available at https://psl.noaa.gov/cgi-bin/data/composites/printpage.pl) is used to plot composite maps. For atmospheric circulation data (vector wind at 850-hPa), the NCEP/National Center for Atmospheric Research (NCAR) reanalysis was used (Kalnay et al. 1996 and references therein). This 850-hPa level is known to be a good indicator of broad-scale features of low-level winds.

Monthly average rainfall data: The station-based observed rainfall data (1950–2004) are from the NCEI data portal and the most recent rainfall data (2005–2019) from the PEAC-monthly conference call summary report (available at https://www.weather.gov/peac/PEAC_Monthly_Call). The National Weather Service (NWS) field offices at the USAPIs are the primary source of this rainfall data, which is collected daily from different rain-gauge stations. The PEAC Center continuously monitors the station-based monthly rainfall information for each of the islands. The island-wide annual rainfall standard deviation ranges from 42 to 110 mm with Chuuk being the lowest at 42 mm and Guam the highest at 110 mm. Other islands such as Saipan, Palau, Yap, Pohnpei, Kosrae, Majuro, Kwajalein, and Pago Pago showed values of 100, 90, 97, 69, 50, 56, 85, and 73 mm, respectively.

As a measure of uncertainty, the standard deviation of October–June rainfall on each island for each of the El Niño types has been computed. For the EPE, the variability runs from 64 to 134 mm with the largest one at Kosrae and smallest at Chuuk, which indicates that the spread is largest at Kosrae and smallest at Chuuk. For the CPE, the variability runs from 60 to 108 mm with the largest one at Pohnpei and smallest at Palau. Similarly, for the ME the variability is 79–164 mm with the largest at Kosrae and smallest at Yap.

Monthly mean sea-level data: The research quality monthly (January to December 1970–2019) sea-level data were downloaded from the web site of University of Hawaii Sea Level Center (UHSLC) (https://uhslc.soest.hawaii.edu/). These observed tide-gauge data are used in the PEAC Monthly Conference Call. The Tidal Epoch is defined as the period 1983–2001 and the climatological seasonal cycles are removed from the data. The record was at least 80% complete with no more than five missing years and no more than three consecutive missing years (also see Kruk et al. 2013). The missing values were replaced by the best "nearest neighboring stations", provided the time-series of the two stations are found to be highly correlated and statistically significant. American Samoa (Pago Pago) is the exception due to a level shift of ~ 127 mm during an earthquake in September 2009. An adjustment was made to the current tide-gauge values for Pago Pago

to compensate for the level shift. The island-wide standard deviation of sea-level variability lies between 64 and 110 mm with the largest one at Palau and smallest one at Majuro. The standard deviation for Guam, Yap, Pohnpei, Kwajalein, and Pago Pago are 92, 109, 83, 75, and 93 mm, respectively.

While the calculation of global mean sea level from tide gauges is not straightforward due to a number of considerations, including local and regional changes in winds and ocean circulation, and the lack of a common datum across tide-gauge sites. As a measure of uncertainty, the standard deviation of October–June sea level at each island for each of the El Niño types has been computed. For the EPE, the variability runs from 47 to 139 mm with the largest one at Palau and smallest at Guam, which indicates that the spread is largest at Palau and smallest at Guam. For the CPE, the variability runs from 15 to 34 mm with the largest one at Palau and smallest at Pago Pago. The variability runs from 27 to 68 mm during an ME event with the largest value at Palau and smallest at Kwajalein. The uncertainty in sea level as measured by the spread is much smaller during the CPE events.

3 El Niño simulation from CMIP5 models

The CMIP5 model-based study (Taylor et al. 2012) provides a strong message about the increased risk of extreme El Niño conditions (see Guojian et al. 2017 and references therein) for future generations and demonstrates that both the frequency and intensity of the strong El Niño events increase significantly if the projected central Pacific zonal sea surface temperatures (SST) gradients become enhanced. The studies revealed that the frequency of extreme El Niño events doubles under the 1.5 °C Paris target and could occur roughly every 10 years instead of every 20 (Guojian et al. 2017; Cai et al. 2014; Cai et al. 2015a; Cai et al. 2015b; Weare 2013, and references). Wang et al. (2019) and other studies (see Power et al. 2017 and references) also noted that there is a tendency for the frequency of both El Niño and La Niña to increase in the future (also see Timmermann et al. 1999; Guojian et al. 2017; and Cai et al. 2021). However, as per multi-model output (see Guojian et al. 2017 and references therein), there is little to no change of La Niña under 1.5 °C or 2 °C warming. This means a greater likelihood of more intense El Niño-related impacts on the USAPIs in the near future. This will not be discussed in any more detail as this has already been addressed in many other papers (see Guojian et al. 2017; Cai et al. 2014; Cai et al. 2015a; Cai et al. 2015b; Weare 2013; Wang et al. 2019; Power et al.

2017; Timmermann et al. 1999; and Cai et al. 2021 and references therein).

4 An overview of different types of El Niño

Studies have shown that El Niño has different "flavors" (Larkin and Harrison 2005; Ashok et al. 2007; Kug et al. 2009) and they are primarily classified on the basis of spatial patterns of the SST and, sometimes, wind anomalies.

A composite of SST and low-level wind anomalies of EPE, ME, and CPE types of El Niño events during 1970–2019 is presented in Fig. 2, and the years of occurrences of these events are summarized in Table 1.

Note that the classification of El Niño events (Table 1) is primarily based on Kug et al. (2009). The three groups of El Niño are classified based on the zonal location of the equatorial SST. Some El Niño events show stronger SST anomalies in the eastern Pacific and are characterized by relatively large SST anomalies in the Niño-3 region (5° S–5° N, 150°–90°

SST (EPE)   Wind (EPE)

(ME)   (ME)
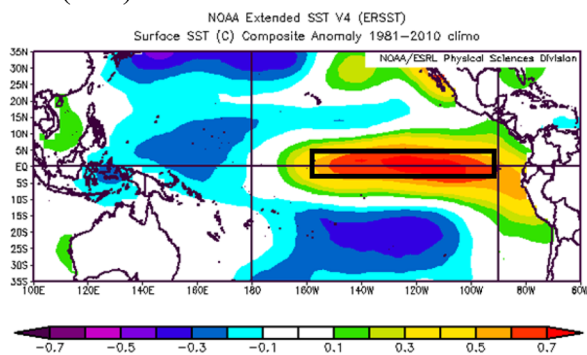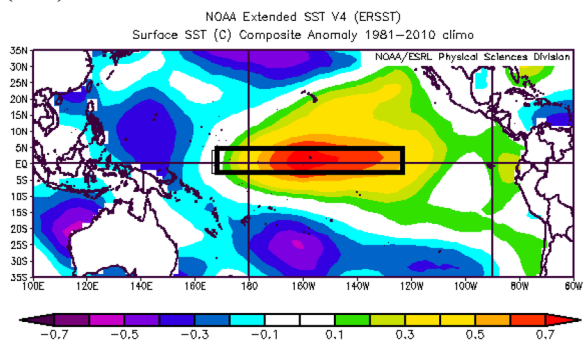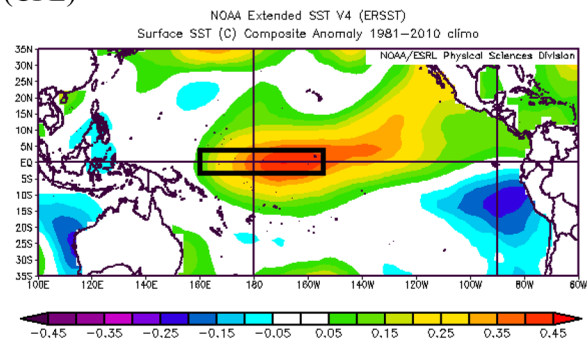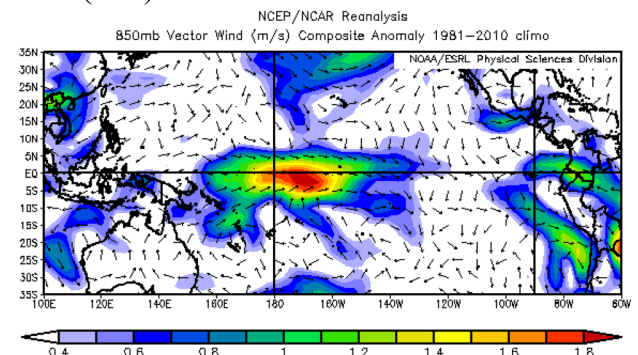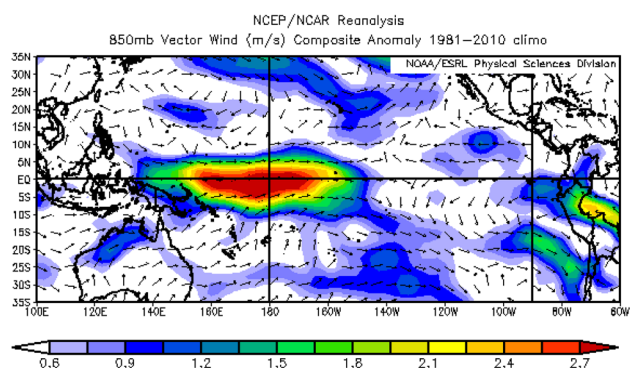
(CPE)   (CPE)
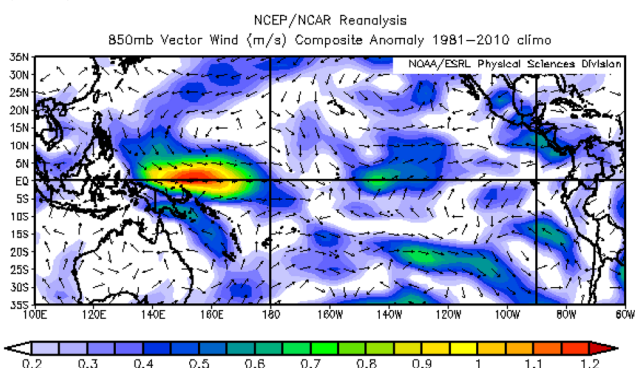
Fig. 2 Composites of SST (°C) (left) and 850-hPa vector wind (m/s) (right) anomalies of El Niño events during 1970–2019 (note that 1981–2010 is the climatological period). The anomalies are averaged from September to the following February (SONDJF) and computed for the year clusters listed in Table 1. The El Niño events are classified into EPE (top), ME (middle) and CPE (bottom). The black boxes (left panel) indicate Niño-3 (top), Niño-3.4 (middle), and Niño-4 (bottom)

Table 1 Years of EPE, ME, and CPE events

	Eastern Pacific El Niño (EPE) (Niño-3 region) 5° S–5° N, 90–150° W)	Mixed El Niño (ME) (Niño-3.4 region) (5° S–5° N, 170–120° W)	Central Pacific (CPE) (Niño-4 region) 5° S–5° N, 160° E–150° W
	1972–73	1986–87	1977–78
	1976–77	1987–88	1990–91
	1982–83	1991–92	1994–95
	1997–98		2002–03
	2015–16		2004–05
			2009–10
			2018–19

The SST anomalies are averaged from September to the following February. (In addition, see Kug et al. 2009)

W). These are classified as EPE and include the events in 1972–73, 1976–77, 1982–83, 1997–98, and 2015–16. Note that the SST pattern of the EPE events is quite similar to that of the conventional El Niño. However, unlike the EPE, some El Niño events have larger SST anomalies in the central Pacific Niño-4 region (5° S–5° N, 160° E–150° W). These are CPE and the events in 1977–78, 1990–91, 1994–95, 2002–03, 2004–05, 2009–10, and 2018–19 fall into this group. There is another type of El Niño which shows the maximum SST anomalies in between 120° and 150° W. These are ME events and 1986–87, 1987–88, and 1991–92 fall into this group.

The EP type of El Niño is associated with the basin-wide thermocline and surface wind variations. Its largest SST anomalies are in the eastern equatorial Pacific (Fig. 2, left/top) and then propagate westward to the equatorial central Pacific (Rasmusson and Carpenter 1982). The CPE events have their largest SST anomalies centered in the central equatorial Pacific (Fig. 2, left/bottom) and their propagating features are less clear (Kao and Yu 2009). In particular, the thermocline variations appear to exert less influence on the CPE type and zonal advection feedback and air-sea heat fluxes become more important for the central Pacific SST anomalies (Kug et al. 2009; Kao and Yu 2009; Newman et al. 2011). The CPE type may also be driven by atmospheric forcing from the subtropical North Pacific by the footprinting mechanism (Vimont et al. 2003). The subtropical atmospheric circulation can first induce positive SST anomalies off Baja California during boreal winter, which then spread southwestward in the following seasons through the subtropical atmosphere–ocean interaction and reach the tropical central Pacific to yield a CPE (Kim and Yu 2012; Paek et al. 2017). The ME (Fig. 2, left/middle) event is characterized by a SST pattern in which the maximum anomalies are located south of Hawaii, in the center of the Nino3.4 domain.

It is important to note that during EPE events, the Aleutian low deepens and shifts equatorward, bringing an anomalous northwesterly flow to the subtropical eastern North Pacific (Fig. 2, right/top). Of relevance to the USAPI is the establishment of anticyclonic anomalies over the Philippines Sea. The presence of the anticyclone suppresses convection, which contributes to low rainfall and drought in the western Pacific islands (Yu et al. 1997; Ludert et al. 2018). Westerly wind anomalies emerge in the equatorial Pacific early in the year and extend eastward to 120 W during Sep–Feb. Similarly, for ME, the Aleutian low deepens but the Philippine Sea anticyclone is replaced by a weak cyclonic circulation (Fig. 2, right/middle). The equatorial westerly anomalies are strongest during the mixed events and centered near the dateline. In contrast, for the CPE events, the anomalous cyclonic flows over the western Pacific are conspicuous and wide spread. As a result, the band of maximum equatorial westerlies is confined to near 150° E (Fig. 2, right/bottom), which is westward relative to EPE and ME. The following section provides an update of island-wide month-by-month rainfall and sea-level variability during EPE, ME, and CPE events.

5 El Niño impacts on the USAPIs

Climatologically, easterly trade winds prevail in the tropical Pacific from a region of high pressure over the eastern extent of North and South Pacific basins toward a region of low pressure in the western Pacific. Since surface winds in the tropics mainly follow the pressure gradient, easterly winds prevail. The easterly winds not only induce equatorial Ekman upwelling because of the Coriolis effect, creating a cold tongue in the equatorial eastern Pacific, but they also raise sea level in the west and lower it to the east.

Wyrtki (1975) found that in the year before an El Niño occurred, trade winds strengthened, increasing the zonal gradient of sea level across the tropical Pacific by building up the water in the western Pacific. Any prolonged relaxation of central Pacific trade winds would then lead to a dynamical consequence in which the accumulated western Pacific warm water and high sea level would not be maintained under a reduced zonal sea-level gradient, and thus would

travel eastward as a wavelike body known as oceanic Kelvin waves, deepening the thermocline and raising the sea level and sea surface temperature of the eastern equatorial Pacific (Delcroix et al. 1991).

Some of the USAPIs have experienced El Niño-related drought (Yu et al. 1997; Ludert et al. 2018) and La Niña-related flooding (Chowdhury and Chu 2019). Specifically, the low-lying atolls in the Federated States of Micronesia (FSM) and Republic of Marshals Islands (RMI) are particularly vulnerable to El Niño-related lower rainfall, lower sea level, and related heat stress. La Niña-related heavy rainfall and higher sea levels can cause flooding disruptions to these islands as well. This is a major concern as the sea level in the USAPI region is highly sensitive to ENSO, with low sea level (on an average 50–150 mm lower than normal) during El Niño years and high sea level (on an average 50–150 mm higher than normal) during La Niña years (Chowdhury et al. 2007; Chowdhury et al. 2014; Chowdhury and Chu 2015; also see Becker et al. 2012).

A recent study by Freund et al. (2019) demonstrated that El Niño events differ substantially in their spatial pattern, intensity, and impacts on the location and intensity of temperature and precipitation anomalies globally. Fang and Mu (2018) noted that while the simple zonal two-region framework of the recharge paradigm can accurately manifest the EPE, it cannot fully depict the variations of the CPE. This is because of the difference in locations of the major warming centers, which are located in the eastern Pacific during the EPE (Fig. 2, left/top) and central Pacific during the CPE (Fig. 2, left/bottom) events. Wang et al. (2019) hypothesized that this regime change arises from background warming in the western Pacific and associated increased zonal sea surface temperature (SST) gradients in the equatorial central Pacific, which reveals a controlling factor that could lead to increased extreme El Niño events in the future. To overcome the future challenges of hazard management in the USAPIs, the island-specific physical interpretations of different El Niño impacts on rainfall and sea level are critical.

5.1 Seasonal rainfall variability

Previous studies (Yu et al. 1997; Ludert et al. 2018) confirmed that the rainfall variations in the USAPIs are significantly distinct in El Niño and La Niña years, and the change in El Niño rainfall is different from a non-El Niño year. The ENSO-related variations in trade winds strongly influence the western extremity of the Pacific (Collins et al. 2011). Ludert et al. (2018) showed that rainfall anomalies have different relationships to ENSO for the USAPIs. Murphy et al. (2014) showed that the three types of El Niño produce different rainfall impacts across the tropical Pacific island countries.

Figure 3 shows the observed rainfall pattern across the USAPI during different El Niño types. It is clear that during the EPE events (Fig. 3, top), all northwestern Pacific (NWP) islands displayed significantly lower than normal rainfall (on average 40–80% below) from October (El Niño 0 or the year of onset of the event) to the following May (El Niño + 1), and it statistically significant from non-El Niño years. Only one south Pacific USAPI (Pago Pago in American Samoa) also displayed lower than average rainfall with exceptions around the month of December and following April, where it shows near normal rainfall. The ME events (Fig. 3, middle) show an erratic trend for all NWP islands during October to January. Any definitive conclusion for this trend is a subject for further study. Interestingly, unlike Murphy et al. (2014), a clear pattern of lower than normal rainfall (on average 20–60% below) is noticeable in the same NWP region from February to May (El Niño +1). The SP islands (Pago Pago in American Samoa) displayed similar EPE like trend with weaker magnitude and some exceptional high peaks (40–70% above) during the month of December and April. The CPE types (Fig. 3, bottom) show that many NWP islands recorded higher than normal rainfall and wetter (on average 20–60% above rainfall) from January to April (El Niño +1). The south Pacific station also displayed a similar wet pattern from October (El Niño 0) to May (El Niño +1). Therefore, the EPE events are associated with drier than normal rainfall from October of the El Niño developing year to May of the following year because of the dominance of anticyclonic anomalies in the western Pacific islands. Wetter than normal rainfall is generally observed from January to April of the year following an El Niño event during the CPE events. This wet period is rather short (4 months) relative to the long-lasting drought (8 months) observed during the EPE events. In the ME event, the entire USAPI did not show any sign of drought until February of the following year and the lower than normal rainfall continued through the following May.

5.2 Seasonal sea-level variability

The anomalous low-level wind generates an anomalous oceanic state in the tropical Pacific Ocean and, as a result, variations in sea-level height occur. Using observational data, Fig. 4 shows sea-level anomalies during the EPE (top), ME (middle), and CPE (bottom) events.

For the EPE composite, with the reduction of equatorial easterlies in the form of weak westerly anomalies (Fig. 2) over the equatorial western Pacific, negative sea-level anomalies start from September of El Niño 0 (the year of onset for El Niño) and all North Pacific stations stay significantly below normal until the following March (Fig. 4, top). After March, there is a slight rise and after April some North Pacific stations (e.g., Palau, Pohnpei, Majuro, and

Fig. 3 Monthly observed mean rainfall anomalies in the USAPIs during EPE (top), ME (middle), and CPE (bottom) events (1975–2019) (Y-axis: rainfall anomaly in %, X-axis: months) (Note that the Y-axis scale for each panel is different from the others). (Data Source: PEAC's monthly conference call note available at https://www.weather.gov/peac/PEAC_Monthly_Call, accessed on March 21, 2019)
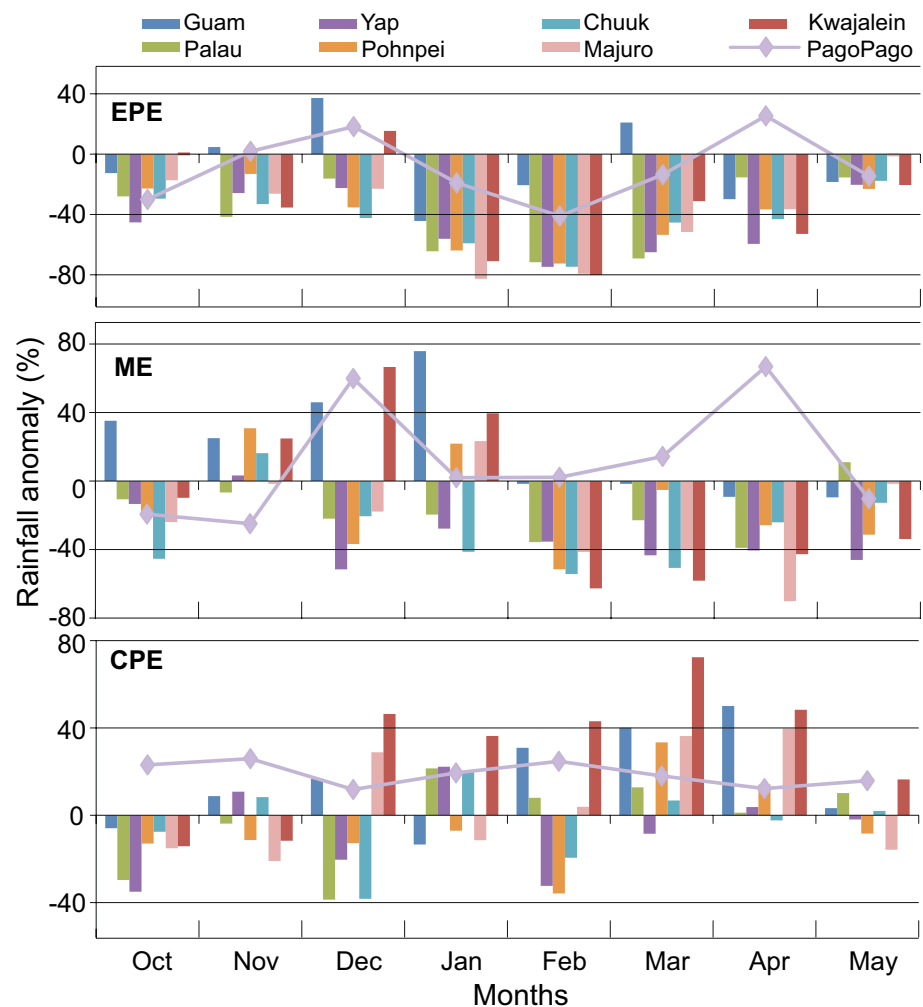
Kwajalein) start to show near normal or positive anomaly while Guam still stays marginally below normal. This is due to the eastward movement of equatorial westerly anomalies and reversal of the prevailing wind direction between 160° E and 160° W (Fig. 2, top/right panel) (Chowdhury et al. 2007).

The ME (Fig. 4, middle) events display a pattern similar to EPE (i.e., lower than normal sea level) but with some noticeable exceptions. For example, while the sea level during EPE events stays significantly below normal with a positive slope in time (not shown but is on average 200–50 mm below) from October to March (Fig. 4, top), the ME events display a concurrent negative slope (not shown but is on average 20–150 mm below) from October to April. In the case of ME, considerably lower than normal (50–150 mm below) sea level did not occur until December and is delayed by 2 months relative to EPE events.

For the CPE events, both the RMI stations (e.g., Majuro and Kwajalein) in the eastern extreme of the NWP display positive anomalies from September of El Niño 0 to the following May (Fig. 4 bottom). This is consistent with Kug

et al. (2009) who reported that during CPE the positive sea-level anomaly is located over the central Pacific (maximum near 150° W). One of the FSM stations (Pohnpei) stays near normal from October to February, followed by positive anomalies from March to June. The other three stations (Guam, Palau and Yap) show significant negative anomalies (25–100 mm below) until the following April.

The other interesting point is the response from the South Pacific islands during EPE events. While the North Pacific islands show negative anomalies from October, Pago Pago's negative anomalies do not appear until January (Fig. 4, top). This is attributed to the changing location of surface westerly winds during the evolution of an EPE episode. This wind causes the North Pacific islands to record negative sea level from July to December. As the season advances, the band of westerly winds moves eastward and causes American Samoa (Pago Pago) to show negative sea-level anomalies from January to June of El Niño + 1 with a six month time lag as compared to Guam and the Marshalls (Fig. 4, top) (Chowdhury et al. 2007). Since the equatorial westerlies are confined in the western

Fig. 4 Same as Fig. 3, except for monthly observed mean sea-level anomaly (SLA) (1975–2019) (Y-axis: sea-level anomaly in mm; X-axis: months) (Note that the Y-axis scale for each panel is different from the others). (Data Source: University of Hawaii Sea Level Center https://uhslc.soest.hawaii.edu/ and PEAC's monthly conference call note available at https://www.weather.gov/peac/PEAC_Monthly_Call, accessed on March 21. Note that there is no tide-gauge station in Chuuk and, therefore, it is not reported here)
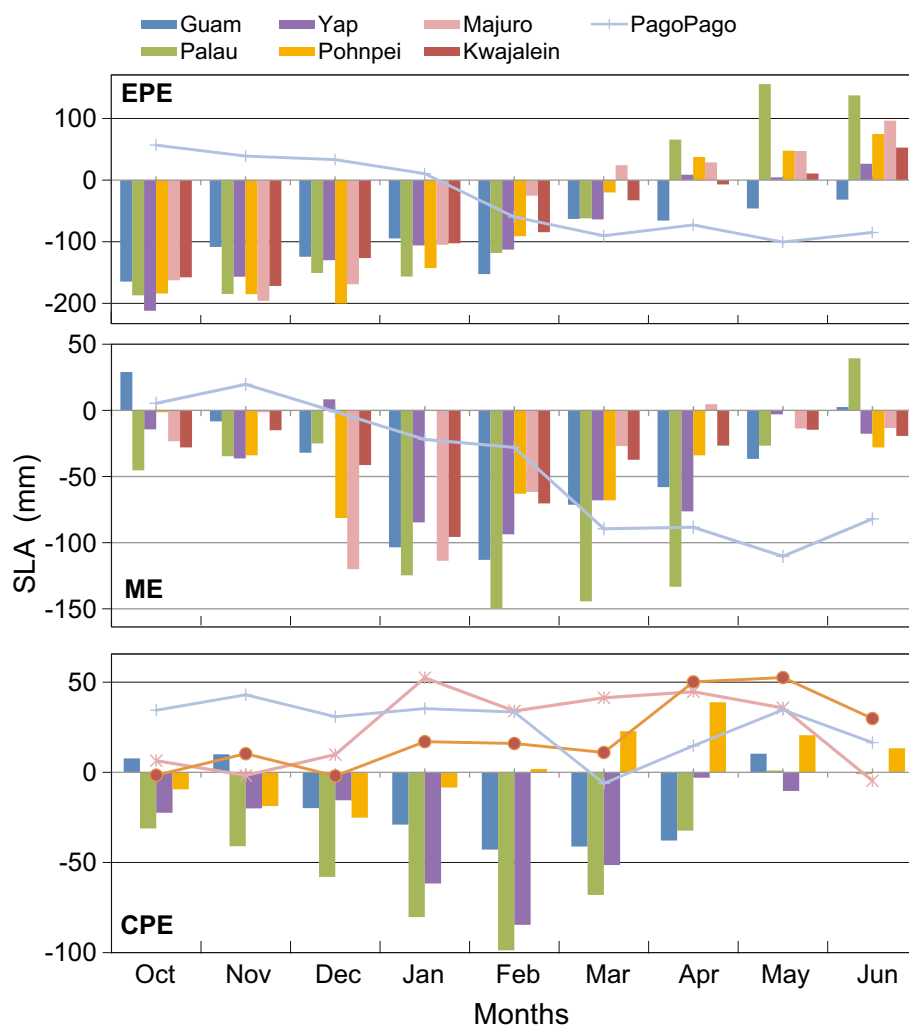
Pacific during CPE (Fig. 2), persistent and negative sea-level anomalies are observed at Palau, Guam, and Yap from December to the following March (Fig. 4, bottom).

Previous studies of Chowdhury et al. (2007) found that the sea-level variations in the tropical Pacific islands are distinct in El Niño and La Niña years. To verify if the current results are statistically significant or not, a non-parametric Mann–Whitney test (Chu and Chen, 2005; Wilks, 1995) was conducted. Because of the smaller sample size for each data batch, a non-parametric test is justified. To verify the contrast between the two extreme events, the two sea-level data batches pertinent to El Niño and non-El Niño (La Niña) years are pooled from the samples. The null hypothesis is that the two batches come from the same distribution. Results indicate that sea-level variability during the El Niño years are different and statistically significant when compared to non-El Niño years. In the north USAPIs, it is statistically significant at the 5% level for

the seasons OND, JFM, and AMJ. Only one of the South Pacific USAPIs, American Samoa (Pago Pago), did not show any clear evidence of significance.

6 Conclusions

Using observational data, we examined rainfall and sea-level variability in the USAPI region. The results show that the classifications of EPE, CPE, and ME adequately depict the different variations of rainfall and sea-level anomalies in the USAPI region (with other modes still possible). The key findings are as follows.

- While the EPE and ME events are associated with lower than normal rainfall (October to June) in the USAPIs, the CPE events are linked to enhanced rain-

fall, particularly from January to April, for most of the islands.

- Similarly, the EPE and ME events are associated with lower than normal sea level in the USAPIs, while the CPE events are linked to higher than normal sea level, particularly from January to May, for some islands (e.g., Majuro, Kwajalein, and Pago Pago).
- With the exception of Pago Pago in American Samoa, the EPE and ME events are associated with dry conditions for the entire USAPIs, however, CPE events are linked to more variability in rainfall with wetter conditions observed at majority of islands.

Current observations already indicate an increasing El Niño trend and, since the late 1990s, the numbers of CPE events have significantly increased relative to EPE events (e.g., Lee and McPhaden 2010; Lu et al. 2020). The recent CMIP5-model-based study (see Guojian et al. 2017 and references therein) also provided a strong message that El Niño events are in the process of becoming more intense in the future. Therefore, the prime concerns for future disruptions in the USAPI region, particularly the water-stressed islands and low-lying atolls in the FSM and RMI, are heavily dependent on the consequences of the increasing frequency of El Niño and related rainfall, sea level, and other climate anomalies. Therefore, information related to island-specific rainfall and sea-level response to different El Niño events is critical to support the short-to-mid-term planning and management activities of the sectors such as water resources, health, fisheries, agriculture, civil defense, public utilities, and coastal zone management in the USAPIs. In conclusion, an improved scientific perspective on the different El Niño flavors (e.g., CPE, ME, and EPE) and their impacts on island-specific rainfall and sea-level anomalies are essential for hazard preparedness actions in the face of the increasing risk of El Niño.

References

Ashok K, Behera SK, Rao SA, Weng H, Yamagata (2007) T. El Niño Modoki and its possible teleconnection. J Geophys Res 112:C11007

Becker M, Meyssignac B, Letetrel C, Llovel W, Cazenave A, Delcroix T (2012) Sea level variations at tropical Pacific islands since 1950. Global Planet Change 80–81:85–98. https://doi.org/10.1016/j.gloplacha.2011.09.004

Cai W et al (2014) Increasing frequency of extreme El Niño events due to greenhouse warming. Nat Clim Change 4:111–116

Cai W et al (2015a) Increasing frequency of extreme La Niña events under greenhouse warming. Nat Clim Change 5:132–137. https://doi.org/10.1038/nclimate2492

Cai W et al (2015b) ENSO and greenhouse warming. Nat Clim Change 5:849–859

Cai W, Santoso A, Collins M et al (2021) Changing El Niño-Southern Oscillation in a warming climate. Nat Rev Earth Environ 2:628–644. https://doi.org/10.1038/s43017-021-00199-z

Chowdhury MR, Chu P-S (2015) Sea level forecast and early warning application—expanding cooperation in the South Pacific. Bull Am Meteorol Soc 96:3381–3386

Chowdhury MR, Chu P-S (2019) A study of the changing climate in the US-affiliated Pacific Islands using observations and CMIP5 model output. Meteorol Appl 26(4):528–541

Chowdhury MR, Chu P-S, Schroeder T (2007) ENSO and seasonal sea level variability—a diagnostic discussion for the U.S.-affiliated Pacific Islands. Theor Appl Climatol 88:213–224

Chowdhury MR, Chu P-S, Guard C (2014) An improved sea level forecasting scheme for hazards management in the U.S.-affiliated Pacific Islands. Int J Climatol 34:2320–2329

Chu P-S (2004) ENSO and tropical cyclone activity. In: Murnane RJ, Liu K-B (eds) Hurricanes and typhoons: past, present, and future. Columbia University Press, New York, pp 297–332

Chu P-S, Chen H (2005) Interannual and interdecadal rainfall variations in the Hawaiian Islands. J Climate 18:4796–4812

Collins D, Sen Gupta A, Power S (2011) Observed climate variability and trends. In: Cambers G, Hennessy K, Power S (eds) Climate change in the Pacific: scientific assessment and new research: regional overview, vol 1. CSIRO, Canberra, pp 51–77

Delcroix T, Picaut J, Eldin G (1991) Equatorial Kelvin and Rossby waves evidenced in the Pacific Ocean through geosat sea-level and surface current anomalies. J Geophys Res 96:3249–3262

Fang X-H, Mu M (2018) A three-region conceptual model for central Pacific El Niño including zonal advective feedback. J Climate 31:4965–4979. https://doi.org/10.1175/JCLI-D-17-0633.1

Freund MB, Benjamin JH, David JK, Helen VM, Nerilie JA, Dietmar D (2019) Higher frequency of central Pacific El Niño events in recent decades relative to past centuries. Nat Geosci 12:450–455. https://doi.org/10.1038/s41561-019-0353-3

Guojian W et al (2017) Continued increase of extreme El Niño frequency long after 1.5°C warming stabilization. Nat Clim Change 7(8):568–572. https://doi.org/10.1038/nclimate3351

Irving D et al (2011) Evaluating global climate models for the Pacific Island region. Clim Res 49:169–187

Kalnay E et al (1996) The NCEP/NCAR 40-year reanalysis project. Bull Am Meteorol Soc 77(3):437–472

Kao HY, Yu J-Y (2009) Contrasting eastern-Pacific and central-Pacific types of ENSO. J Climate 22:615–632

Kelman I (2019) Pacific island regional preparedness for El Niño. Environ Dev Sustain 21:405–428. https://doi.org/10.1007/s10668-017-0045-3

Kim ST, Yu J-Y (2012) Examination of the two types of ENSO in the NCEP CFS model and its extratropical associations. Mon Weather Rev 140:1908–1923

Kruk MC, Marra JJ, Ruggiero P, Atkinson D, Merrifield M, Levinson D, Lander M (2013) Pacific storms climatology products: understanding extreme events. Bull Am Meteorol Soc 94(1):13–18

Kug J-S, Jin F-F, An S-I (2009) Two types of El Niño events: cold tongue El Niño and warm pool El Niño. J Climate 22:1499–1515. https://doi.org/10.1175/2008JCLI2624.1

Lander MA (1994) An exploratory analysis of the relationship between tropical storm formation in the western north Pacific and ENSO. Mon Weather Rev 122:636–651

Larkin N K, Harrison DE (2005) Global seasonal temperature and precipitation anomalies during El Niño autumn and winter. Geophys Res Lett 32:L16705

Lee T, McPhaden MJ (2010) Increasing intensity of El Niño in the central-equatorial Pacific. Geophys Res Lett 37:L14603. https://doi.org/10.1029/2010GL044007

Lu B, Chu P-S, Kim S-H, Karamperidou C (2020) Hawaiian regional climate variability during two types of El Niño. J Climate 33(22):9929–9943

Ludert A, Wang B, Merrifield M (2018) Characterization of dry conditions across the US-affiliated Pacific Islands during near-neutral ENSO phases. J Climate 31(16):6461–6479

Marler TE (2014) Pacific island tropical cyclones are more frequent and globally relevant, yet less studied. Front Environ Sci 2(42):1–6. https://doi.org/10.3389/fenvs.2014.00042

Murphy BF, Power SB, McGree S (2014) The varied impacts of El Niño-Southern Oscillation on Pacific island climates. J Climate 27:4015–4036. https://doi.org/10.1175/JCLI-D-13-00130.1

Newman M, Alexander MA, Scott JD (2011) An empirical model of tropical ocean dynamics. Clim Dyn 37:1823–1844

Paek H, Yu J-Y, Quian C (2017) Why were the 2015/2016 and 1997/1998 extreme El Niños different? Geophys Res Lett 44:1848–1856. https://doi.org/10.1002/2016GL071515

Power SB et al (2017) Humans have already increased the risk of major disruptions to Pacific rainfall. Nat Commun 8(14368):1–7. https://doi.org/10.1038/ncomms14368

Rasmusson EM, Carpenter TH (1982) Variations in tropical sea surface temperature and surface wind fields associated with the Southern Oscillation/El Niño. Mon Weather Rev 110:354–384

Taylor KE, Stouffer RJ, Meehl GA (2012) An overview of CMIP5 and the experiment design. Bull Am Meteorol Soc 93:485–498

Timmermann A, Oberhuber J, Bacher A et al (1999) Increased El Niño frequency in a climate model forced by future greenhouse warming. Nature 398:694–697. https://doi.org/10.1038/19505

Vimont DJ, Wallace JM, Battisti DS (2003) The seasonal footprinting mechanism in the Pacific: implications for ENSO. J Climate 16:2668–2675

Wang B et al (2019) Historical change of El Niño properties sheds light on future changes of extreme El Niño. Proc Nat Acad Sci. https://doi.org/10.1073/pnas.1911130116

Weare B (2013) El Niño teleconnections in CMIP5 models. Clim Dyn 41:2165–2177

Wilks DS (1995) Statistical methods in the atmospheric sciences. Academic Press, Cambridge, p 467

Wyrtki K (1975) El Niño—the dynamical response of the ocean to atmospheric forcing. J Phys Oceanogr 5:572–584

Yu Z-P, Chu P-S, Schroeder T (1997) Predictive skills of seasonal to annual rainfall variations in the U.S. affiliated Pacific islands: canonical correlation analysis and multivariate principal component regression approaches. J Climate 10:2586–2599